JOURNAL OF SOLID STATE CHEMISTRY **96**, 301–310 (1992)

As_xSe_{1-x} System ($0.20 \leq x \leq 0.57$): EXAFS Study of the Glass Region

V. MASTELARO,*[†] H. DEXPERT,[†] S. BENAZETH,[†][‡]
AND R. OLLITRAULT-FICHET[‡]

[†]LURE, CNRS-CEA-MEN, Université Paris XI, 91405 Orsay Cedex, France; and [‡]Lab. de Chimie Minérale et Structurale—Université Paris V, 75270 Paris Cedex, France

Received May 15, 1991

We have examined the local structure of the As_xSe_{1-x} ($0.20 \leq x \leq 0.57$) system by Extended X-Ray Absorption Fine Structure (EXAFS) measurements. The two atoms have been successively excited, with both showing a unique contribution for their radial distribution function. At the arsenic *K* edge, the one shell fit is consistent with the presence of pyramidal $AsSe_3$ building units, bridged by selenium atoms, as indicated by the data analyzed at the selenium *K* edge. The evolution of the Debye–Waller factor at the arsenic *K* edge is discussed as well as the variation of the Se–As distance observed at the selenium edge, both phenomena depending on the arsenic composition. These effects can be explained by the existence of some As–As and Se–Se homopolar bonds in the arsenic- and selenium-rich glasses, respectively. The Fourier transform magnitude from the data collected at 35 K at the arsenic *K* edge does not show other shells than the first As–Se principal peak. The qualitative interpretation of the XANES part of the absorption spectra is in good agreement with the present structural investigation.

I. Introduction

The study of the local order existing in the amorphous semiconductors is very important for understanding their specific physical properties, and EXAFS (*1*, *9*), infrared, Raman, X ray and neutron diffraction measurements (*2–8*) have been extensively employed. These results, resumed in Table I, are as follows:

G. Lucovsky *et al.* (*2*) have shown that the infrared and Raman spectra of the amorphous As_xSe_{1-x} ($0.40 \leq x \leq 0.60$) are well described by the vibration of the $AsSe_3$ stretching mode. The analysis of the infrared and Raman spectra indicates that the 8-*N* coordination rule applies at all glassy compositions, and that heteropolar bonds are always favored. The infrared and Raman spectra for the arsenic-rich region does not show, relative to the stoichiometric composition, a significant difference as they observed for the As_xS_{1-x} system; this is explained by the large similarities of the physical properties presented by the As and Se atoms. Moreover, the authors conclude that the tendency toward ordering is less in the As-rich region.

Later on, still using Raman, T. Mori *et al.* (*3*) showed that in the selenium-rich region of the As_xSe_{1-x} ($0 \leq x \leq 0.5$) system, $AsSe_3$ pyramids always exist as fundamental struc-

---

* To whom correspondence should be addressed.

0022-4596/92 $3.00

TABLE I

MAIN RESULTS FOUND BY OTHERS' WORKS

Compositions	Se-rich	As-rich		Molecular models propositions	Form	Techniques	References
	Se_8 rings Se chains	As_4Se_4	As_2Se_3				
$0.40 \leq x \leq 0.50$	—	no	$AsSe_3$ units	$AsSe_2As$ $AsSeAs_2$ $AsAs_3$	Bulk	IR, Raman	(*2*)
$0.00 \leq x \leq 0.50$	Yes	no	$AsSe_3$ units	As_2Se_4	Bulk	Raman	(*3*)
$0.00 \leq x \leq 0.50$	—	yes	$AsSe_3$ units	—	Bulk	X-ray diffraction	(*4*)
$0.30 \leq x \leq 0.50$	—	—	$AsSe_3$ units	—	Bulk	X-ray and neutron diffraction	(*5*)
$0.30 \leq x \leq 0.50$	—	yes	$AsSe_3$ units	As_3Se As_3Se_3	Bulk	Monte Carlo simulation	(*7, 8*)
$0.30 \leq x \leq 0.50$	—	yes	$AsSe_3$ units	—	Thin films	Modelization	(*7, 8*)
$0.40 \leq x \leq 0.50$	—	no	$AsSe_3$ units	—	Thin films	X-ray diffraction	(*6*)
0.50	—	—	—	—	Thin films	EXAFS	(*9*)

tural units since the As–Se bond is stable in energy. As the selenium content is increased, the number of Se–Se bonds becomes greater. In the region between stoichiometric As_2Se_3 and pure selenium, the $AsSe_3$ units and Se–Se bonds are distributed homogeneously and randomly in space. They suppose in this case the existence of Se–Se bonds along As–Se–Se–As chains. However, since the frequency of this mode is similar to that of the stretching mode of the $AsSe_3$ pyramidal unit, the identification of the Se–Se stretching mode is difficult. For the arsenic-rich region, when the arsenic concentration is increased relative to the stoichiometric As_2Se_3 composition, the number of As–As bonds due to the extra arsenic atoms grows. They suggest then that the As_2Se_4 structural type may be constructed.

The atomic radial distribution functions of the As–Se glasses have been studied by A. L. Renninger and B. L. Averbach (*4*) in the As_xSe_{1-x} glasses with $0.0 \leq x \leq 0.5$. They found that the first neighbor correlation peak shifts linearly from 2.34 Å for pure selenium to 2.41 Å for $x = 0.36$ and remains constant at higher arsenic concentration. Peak areas increase linearly with arsenic concentration and their magnitudes agree well with a model which assumes that selenium is twofold coordinated and that arsenic is threefold coordinated. Moreover, they found that at $x = 0.40$ and $x = 0.50$ the first and second neighbor peaks are very similar to that obtained from the crystals As_2Se_3 and As_4Se_4. This suggests that local crystalline configurations, possibly made of $AsSe_3$ units and As_4Se_4 molecules, also exist in the bulk glasses. However, significant differences between the crystalline and amorphous distributions are observed after the second peak. They conclude then that models based on the existence of microcrystalline regions of As_2Se_3 and As_4Se_4 observed for those two compositions do not give satisfactory agreement with the experimental distributions.

Later on, A. J. Leadbetter and A. J. Apling (*5*) studied the As_xSe_{1-x} ($0.30 \le x \le 0.50$) glasses by X-ray and neutron diffraction. They showed that for selenide glasses the sheet structure becomes more pronounced when increasing the arsenic concentration. For all the glasses, the data are consistent with full satisfaction of the respective two- and threefold covalency requirements of chalcogenide and arsenic atoms. The distribution of arsenic–chalcogenide bond lengths is shown to be symmetrical about the average values of 2.44 Å.

The structure of differently prepared vacuum deposited As_2Se_3 films and As_2Se_3 and As_2Se_2 melt-quenched glasses have been investigated by J. Notholt and J. Liese (*6*) using X-ray diffraction experiments. For all the films they studied, no significative structural variations were observed: the structure remained similar to the As_2Se_2 glass composition. Moreover, it is impossible to find a distinct peak due to the As–As distance in the correlation functions, and they observed that the As–As bonding existence just yields an increase of the halfwidth of the first peak in the As_2Se_2 composition.

A full description about the short and medium range order in chalcogenide alloys can be found in two papers published by J. C. Phillips (*7, 8*). The conditions for the formation of microcrystal or clusters in chalcogenide glasses are well described. Concerning the As_xSe_{1-x} system, an analysis of the variation of the glass transition temperature Tg shows that, for $x = 0.40$, a maximum is observed. This is explained by a competition between As_4Se_4 units and As_2Se_3 cross-linked chains. Those As_4Se_4 molecular units are stable in the gas phase and are always present in evaporated As_xSe_{1-x} films. These molecules can be removed by annealing. The As–As bonds present in these alloys are however very difficult to remove. For bulk glasses, the Monte Carlo model for $As_{0.5}Se_{0.5}$ glass composition shows that the structure should be dominated by As_4Se_4 molecules, but the model contains smaller molecular groupings such as As_3Se and As_3Se_3 embedded in the network.

Recently, S. R. Elliot and A. B. Kolobov (*9*), using EXAFS, compared an amorphous $As_{0.50}Se_{0.50}$ film and the corresponding bulk glass. They found that the local structural changes in the first coordination sphere are relatively insignificant. The arsenic atoms are coordinated by 2.4 selenium atoms with a mean bond length R_{As-Se} equal to 2.40 Å and about 0.7 arsenic atoms with a mean bond length R_{As-As} equal to 2.80 Å. Selenium is coordinated to 1.8 arsenic atoms. The uncertainties in the values of coordination numbers they obtained are estimated to be approximately ±0.5.

The preceding survey indicates, in fact, that this system has thus been investigated either by techniques which give qualitative results regarding the number and the mean bond length of exchanged bonds or, when this is not the case, are limited to a few chemical compositions (Table I). All techniques agree on the fact that $AsSe_3$ is the basic unit for all glassy compositions. However, related to the existence of homopolar bonds for arsenic and selenium rich glasses, a controversy exists about the origin of these bonds: do they come from $AsSe_2As$, $AsSeAs_2$, $AsAs_3$ (*2*), or As_2Se_4 type units (*3*), or from As_4Se_4 molecular units (*4, 7, 8*)? It is thus of interest to study the whole range of compositions. This is what we did by examining the binary As_xSe_{1-x} system with $0.20 \le x \le 0.57$, in order to determine step by step the local structure and if evolutions occur with changes in the composition. The description of this structure is in fact very important for us as we also investigate the atomic arrangement existing in the Ag–As–Se ternary diagram, which presents interesting ionic conduction properties (*10*).

II. Experimental and Data Analysis

A. Sample Preparation

Samples of the As_xSe_{1-x} binary system were prepared by direct mixing of arsenic and selenium elements in convenient proportions. The powders were then placed into quartz vacuum tubes and heated in a furnace at 900°C for about 48 hr to ensure a good homogeneity to the melting process. They were then quenched in cold water before being returned to room temperature. We prepared samples in which compositions correspond to x values of 0.20, 0.25, 0.30, 0.35, 0.40, 0.50, and 0.57. Characterizations made by metallography and X-ray diffraction experiments proved that the samples are respectively homogeneous and do not present crystalline phases, in the limits of sensibility of these techniques. For X-ray absorption studies, samples were ground to fine powders (20 μm in size), and then spread uniformly onto an adhesive tape, used as a support for the absorption measurements which have been made in the transmission mode.

B. Data Collection and Analysis

The transmission measurements were performed at room and low temperatures at LURE-DCI (Orsay), using different spectrometers (EXAFS I station—Si(331) channel cut monochromator, EXAFS III and IV stations—Si(311) double crystal monochromator), with ion chambers as detectors. During the measurements, the synchrotron was typically operating at an energy of 1.85 GeV, with an average beam current of 280 mA. Energy steps were 0.4 eV for XANES measurements and about 2 eV for the EXAFS data collection.

The data, after conventional treatment (*11*), were Fourier transformed using k^3 weighting, a Hanning apodisation function being applied over the 3.0 to 13.0 Å^{-1} range we consider. Using the single scattering theory and the plane-wave approximation, the normalized oscillatory part of the absorption spectra is described as

$$\chi(k) = -\sum_i \frac{N_i}{kR_i^2} F_i(k) \exp(-2\sigma_i^2 k^2)$$

$$\exp(-2R_i/\lambda(k) \sin[2kR_i + \phi_i(k)],$$

where k is the electron wave vector, $F_i(k)$ is the backscattering amplitude from each of the N_i equivalent neighbors of i-type which are located at an average distance R_i from the absorbing atom, σ_i is the Debye–Waller term, $\lambda(k)$ is the mean free path of the photoelectron and $\phi_i(k)$ is the total phase shift including central atom and backscatterer contributions. In order to determine the structural parameters R, N, and σ_i, we used the Fourier filtering method (*11*).

Crystalline samples have been taken as reference compounds in order to obtain the backscattering phases and amplitudes used in the EXAFS fitting procedure. In our studies the standards are the crystalline forms of:

(i) Ag_3AsSe_3 (*12*) (each arsenic atom is surrounded by three selenium at a mean bond length of 2.41 Å),

(ii) As_2Se_3 (*13*) (the selenium atom is coordinated by two arsenic atoms at a mean bond length of 2.41 Å),

(iii) Se (*15*) (the selenium atom has two nearest neighbors at 2.33 Å).

(iv) amorphous and crystalline phases of As (*14, 15*) have also been used; in the amorphous phase, the arsenic atom presents three nearest neighbors between 2.45 and 2.49 Å although in the crystal the arsenic presents three nearest neighbors between 2.49 and 2.51 Å.

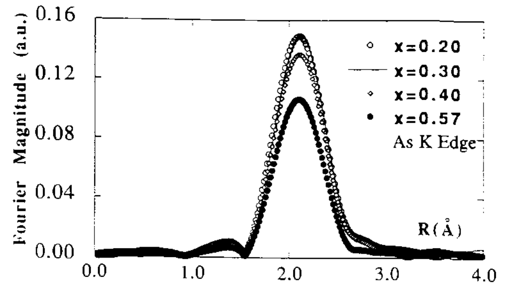

FIG. 1. Fourier transform magnitudes (uncorrected for phase shift) of different As_xSe_{1-x} compositions at the arsenic K edge.

III. Results and Discussion

A. EXAFS Results

Figures 1 and 2 show for some glassy compositions the typical Fourier transform magnitudes at the arsenic and selenium edges obtained at room temperature. These pseudo-radial distribution functions, uncorrected for phase shifts, are quite similar (a unique peak is seen for all the different compositions) when compared with the references compounds, i.e., Ag_3AsSe_3 for the arsenic edge and As_2Se_3 for the selenium data. For a first series of simulation, we consider a one shell model which excludes the existence of homopolar bondings all over the composition range. Figures 3 and 4 show the quality of the adjustment for the real and imaginary components of the Fourier filtered EXAFS (R space) and for the χ (E) EXAFS spectra (E space). We choose to show here the more enriched arsenic (Figs. 3a, 4a) and selenium (Figs. 3b, 4b) glassy compositions ($As_{0.57}Se_{0.43}$ and $As_{0.20}Se_{0.80}$) at the arsenic and selenium edges, regions where homopolar contributions are expected. It is clear that a one shell model could be, in a first approximation, considered good enough to describe the local atomic arrangement of these phases. The number of next nearest neighbors is constant over the whole composition range as shown in Tables II and III either for arsenic or for selenium. The local structure is thus based on threefold pyramidal building units centered on the arsenic atoms and dicoordi-

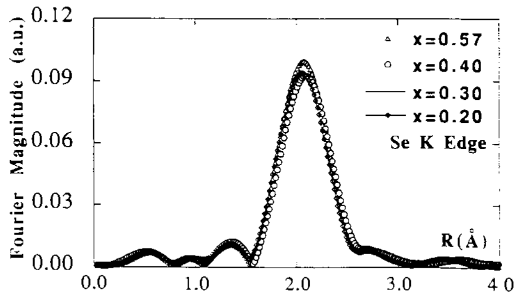

FIG. 2. Fourier transform magnitudes (uncorrected for phase shift) of different As_xSe_{1-x} compositions at the selenium K edge.

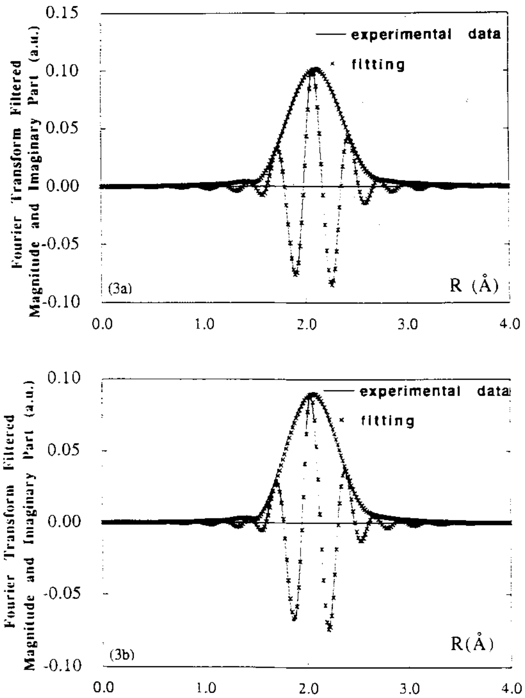

FIG. 3. Typical fitting quality of the magnitude and imaginary part of the Fourier transform without phase correction for (a) $As_{0.57}Se_{0.43}$ at the arsenic edge and (b) $As_{0.20}Se_{0.80}$ at the selenium edge.

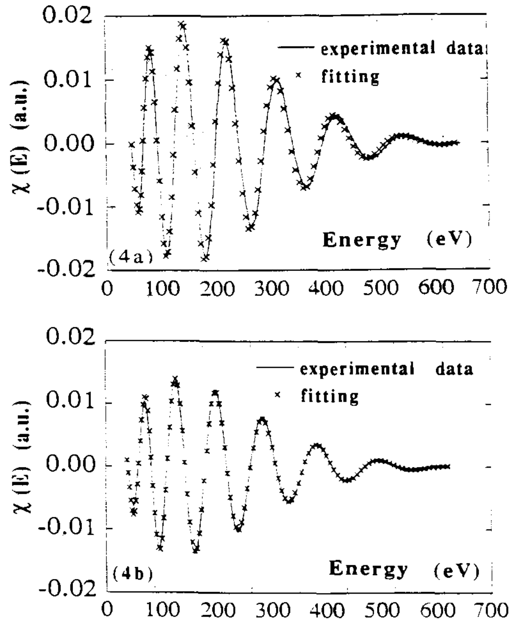

FIG. 4. Typical fitting quality of the χ (E) EXAFS spectra for (a) $As_{0.57}Se_{0.43}$ at the arsenic K edge and (b) $As_{0.20}Se_{0.80}$ at the selenium K edge.

nated selenium atoms. However, several important points come out the data analysis:

(i) If we look carefully over the whole range of results, we find some discrepancies in the evolution of the $\Delta\sigma$ parameter (difference between the Debye–Waller values of the samples and the references). At the arsenic edge (Table II), the fit shows a significant increase for the $\Delta\sigma$ values with the arsenic content. At the selenium edge, however (Table III), the $\Delta\sigma$ values are constant over the entire range of composition. Figure 5 plots these different behaviors.

(ii) Moreover, distances are not equally affected: at the selenium edge, the fit shows a noticeable variation of the Se–As bond length with the arsenic content whereas, at the arsenic K edge, $R_{As\text{-}Se}$ remains unchanged. Figure 6 compares the variation of the $R_{Se\text{-}As}$ and $R_{As\text{-}Se}$ distances as a function of the arsenic content. We must note that the $R_{Se\text{-}As}$ maximum is for the As_2Se_3 stoichiometric composition. We have at this step to explain two questions:

(i) why at the arsenic K edge, in the range

TABLE II

ARSENIC K EDGE: FIT WITH ONE SHELL AT ROOM TEMPERATURE

Composition x% As	$N_{As\text{-}X}$	$R_{As\text{-}X}$ (Å)	$\Delta\sigma_{As\text{-}X}$ (Å)	ΔE (eV)
0.20	2.9	2.41	0.000	−2.2
0.25	3.0	2.41	0.009	−1.5
0.30	3.0	2.41	0.006	−1.4
0.35	2.8	2.41	0.005	−2.0
0.40	2.9	2.41	0.005	−1.7
0.50	2.9	2.41	0.035	−0.8
0.57	3.0	2.41	0.047	−2.3

TABLE III

SELENIUM K EDGE: FIT WITH ONE SHELL AT ROOM TEMPERATURE

Composition x% As	$N_{As\text{-}X}$	$R_{As\text{-}X}$ (Å)	$\Delta\sigma_{As\text{-}X}$ (Å)	ΔE (eV)
0.20	2.0	2.38	0.001	0.1
0.25	2.0	2.39	0.000	0.3
0.30	2.1	2.39	0.000	−0.5
0.35	2.0	2.40	0.000	−0.6
0.40	2.1	2.41	0.000	−0.4
0.50	2.1	2.40	0.000	0.5
0.57	2.1	2.39	0.000	−0.4

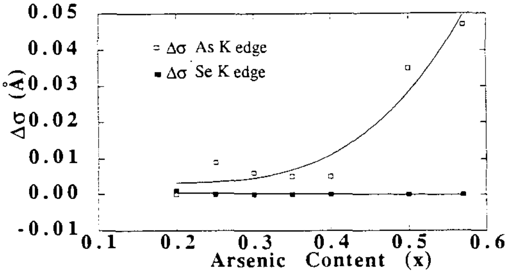

FIG. 5. Variation of the $\Delta\sigma$ parameter with the arsenic concentration at the arsenic and selenium edges.

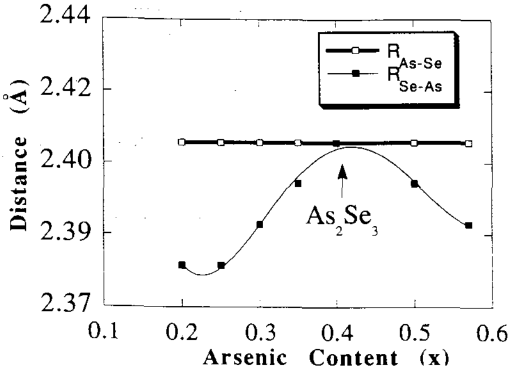

FIG. 6. Variation of the R_{As-Se} and R_{Se-As} mean bond length with the arsenic content.

of the arsenic-rich glasses, does the $\Delta\sigma$ vary while the R_{As-Se} mean bond length remains constant?

(ii) why at the selenium *K* edge, in the region of selenium rich glasses, does the $\Delta\sigma$ remain constant but the R_{Se-As} mean bond length decreases?

As a matter of fact, in this binary system, if only heteropolar bondings exist, we should obtain the same results independent of the arsenic or selenium *K* edges data we collect. The discrepancies we observe indicate that this one shell adjustment is not valid, at least for the regions close to the limits of the system. As–As or Se–Se homopolar bondings may exist but they may not have the same structural behavior.

In order to explain the results at the arsenic *K* edge, for arsenic-rich glasses, we should consider the mean As–Se distance in the stoichiometric phase As_2Se_3 (R = 2.41 Å) and then compare it with the two kinds of distances observed in the crystalline arsenic rich phase As_4Se_4, i.e., R_{As-Se} = 2.38 Å and R_{As-As} = 2.54 Å. If As–As homopolar bonds exist, they would increase the disorder, that means an increase of $\Delta\sigma$, but they will not modify significantly the mean As–*X* (*X* = Se or As) bond length, as the distances As–Se and As–As act in opposite senses. This result is in very good agreement with that found by J. Notholt and J. Liese (*6*).

If we compare our results with those found using EXAFS by C. Y. Yang *et al.* (*16*) on the As_4S_4 glassy composition, we note that on the Fourier transform moduli obtained from the spectra at the arsenic *K* edge, second and third shell peaks exist and are related to the As–As contributions. The distances (2.57 Å for the second peak and 3.54 Å for the third peak) correspond to the intramolecular bonds found in the As_4S_4 molecule. In our case, as we can see in Fig. 1, for all arsenic-enriched compositions we do not observe the apparition of well defined second and third shells, even from low temperature experiments (35K), as shown in Fig. 7. The apparent increase in the magnitude at low temperature is solely due to a strong decrease of the thermal contribution. Thus, although the crystalline phases As_4S_4 and As_4Se_4 are isomorphous (*17*), it is obvious that this is no longer true for the As_4S_4 and As_4Se_4 glassy compositions. This allows us to rule out the existence of As_4Se_4 molecular units in these glasses, as supposed in references (*4, 7, 8*).

At this step, we can suppose that for the As_xSe_{1-x} glass system the origin of As–As homopolar bonds are not the same as for

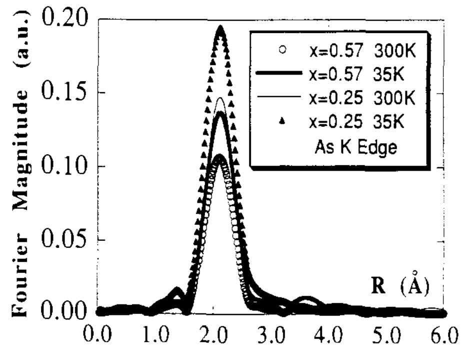

FIG. 7. Fourier transform magnitudes (uncorrected for phase shift) of two glasses at low and room temperature at the arsenic *K* edge.

TABLE IV

ARSENIC K EDGE: FIT USING TWO SHELLS FOR THE $x = 0.57$ GLASSY COMPOSITION

$N_{\mathrm{As-As}}$ initial value[a]	$N_{\mathrm{As-Se}}$	$N_{\mathrm{As-As}}$	$R_{\mathrm{As-Se}}$ (Å)	$R_{\mathrm{As-As}}$ (Å)	$\Delta\sigma_{\mathrm{As-Se}}$ (Å)	$\Delta\sigma_{\mathrm{As-As}}$ (Å)	ΔE (eV)
0.0	3.0	0.0	2.41	0.00	0.05	0.00	−2.5
0.5	2.4	0.5	2.41	2.49	0.04	0.01	−2.6
1.0	1.9	0.9	2.41	2.49	0.03	0.05	−2.6
1.5	1.5	1.5	2.40	2.50	0.01	0.05	−2.6

[a] The total $N_{\mathrm{As-Se}}$ plus $N_{\mathrm{As-As}}$ is considered here equal to three.

those found in the $\mathrm{As}_x\mathrm{S}_{1-x}$ glass system. For example, we cannot throw out:

(i) the existence of clusters of amorphous arsenic;

(ii) the existence of other different units, as suggested by the different works described previously.

If we consider now the selenium K edge results, we must assume that the selenium-rich glasses ($x = 0.20$) are much closer to pure selenium than the arsenic-rich glasses ($x = 0.57$) are to pure arsenic. That means that homopolar bondings may be more numerous in the case of selenium, and their effect must be more important at the selenium edge. The Se–Se homopolar component ($R_{\mathrm{Se-Se}} = 2.33$ Å) tends to decrease the average $R_{\mathrm{Se-}X}$ bond length (X = As or Se), and this is exactly what we observed (Table III).

If we now assume that As–As and Se–Se homopolar bonds exist for enriched arsenic and selenium glasses, respectively, the question is to know if it is reasonable or not to use EXAFS to accurately determine the respective number of these homopolar contributions. We can thus try to match the two shells model (As–Se(As) and Se–As(Se)) with the experimental signal. Before discussing the results of the adjustments, we must define the possible number of independent parameters (N_{pts}) we can use in the two shells fitting procedure. This number is defined as $N_{\mathrm{pts}} = (2\Delta k\Delta R)/\pi$ where Δk is the k space range of the data and ΔR is the width of the window used when Fourier transforming in R space. At the arsenic K edge, $\Delta k = 12.45$ Å^{-1}, $\Delta R = 1.125$ Å, so that $N_{\mathrm{pts}} = 9.0$. This value is therefore the maximum of independent parameters we can adjust simultaneously in the fitting procedure.

Let us now consider the two arsenic-rich compositions $x = 0.50$ and $x = 0.57$: Table IV shows the fitting results for the $x = 0.57$ composition. If all parameters are simultaneously fitted ($N_{\mathrm{pts}} = 7$), the adjustment shows that for both compositions the results are dependent on the (As–Se)/(As–As) ratio, which is defined before the fitting procedure. It is thus very difficult to obtain a quantitative determination of the number of homopolar bonds although their existence is supported. This interpretation does not agree with what Elliot and Kolobov (*9*) said, and EXAFS is definitely not accurate enough to give an exact value of the hetero-polar/homopolar ratio. Moreover, the first As–As mean bond length should be smaller than the distance of 2.80 Å found in their work, simply because it seems hardly possible to separate the As–Se and As–As contributions in the Fourier transform moduli, as shown in Fig. 1.

B. XANES Results

The XANES spectra at the arsenic and selenium K edges show two phenomena:

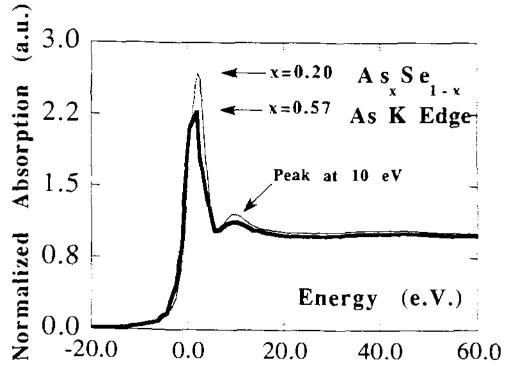

FIG. 8. XANES spectra at the arsenic K edge for $x = 0.20$ and $x = 0.57$ glassy compositions.

(i) a feature at 10 eV above the edge (Fig. 8);

(ii) a variation of the area under the white line related to the arsenic ratio.

For both edges, arsenic or selenium, this area decreases when the arsenic content increases (Fig. 9). J. M. Lee (*18*) observed the same qualitative results for the As–S system.

The full interpretation of XANES results is very difficult because multiple scattering phenomena are involved. However, we recently undertook a theoretical analysis of the As_2Se_3 crystalline phase at the arsenic and selenium edges using the formalism of M. Benfatto and C. R. Natoli (*19*). This analysis may help us to understand the situation existing for the glasses. For the crystalline As_2Se_3 XANES spectra, we observed that:

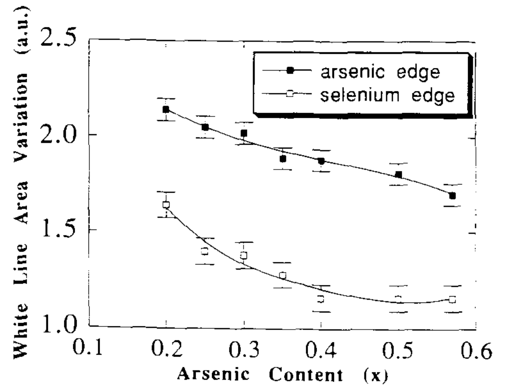

FIG. 9. Variation of the white line area at the arsenic and selenium K edges with the arsenic content.

(i) it is possible to reproduce the feature at 10 eV when we consider the first nine nearest neighbors;

(ii) when an As–As homopolar bond takes the place of an As–Se bond in the first shell, the white line intensity decreases, and the opposite effect is observed when a Se–Se homopolar bond is considered.

From these preliminary calculations, one could suggest a qualitative interpretation of our observations in the glassy compositions. As described above, As–As or Se–Se homopolar bonds have different influences on the mean bond length and lead therefore to different changes for the white line intensity. On the other hand, this intensity also changes for compositions where homopolar bonds are not supposed to exist, indicating that there must be other reasons beside the homopolar bondings for these variations. At this step of our calculation, we can only suggest that in the glasses, where the structure is disordered when compared to the crystalline phase, many other complex phenomena are implied and related to these variations. Further studies are needed in order to better understand this phenomena.

IV. Conclusion

EXAFS has been used to study the atomic arrangement around As and Se in a large area of compositions of the As_xSe_{1-x} system. The analysis of the data allowed us to discuss the existence of homopolar bonds. For the selenium-rich region ($x < 0.40$), the local structure consists of $AsSe_3$ pyramidal units and Se–Se homopolar bonds that may form the Se_n chains or Se_8 rings. On the arsenic-rich region side ($x > 0.40$) the local structure consists of both $AsSe_3$ pyramidal units and As–As homopolar bonds, the origin of which is not yet fully understood. This behavior is different from what has been observed for the arsenic-rich As–S glassy system. The existence of homopolar bonds for enriched selenium and arsenic glasses is in good agreement with the chemical ordering network model issued from other techniques. The similarity of the backscattering phase and amplitude parameters used in the EXAFS analytical procedure is the main limit to a quantitative description based on a two shells model. The XANES qualitative investigation agrees with the EXAFS structural description. The variations in the white line intensity are attributed mainly to changes occurring in the first shell of neighbors.

Acknowledgments

The authors thank the team who ran the machine. We also acknowledge helpful discussions with A. Ibanez and E. Philippot. We are grateful to M. Benfatto and C. R. Natoli for providing and helping to run XANES simulations programs. One of us (V. M.) is supported by a Ph.D. fellowship from CAPES, delivered by the Brazilian government.

References

1. W. W. Cai, G. S. Lin, and C. Yu, *Acta Phys. Sin.* **35**(9), 1164 (1986).
2. G. Lucovsky, F. L. Galeener, R. H. Geils, and R. C. Keezer, *in* "The Structure of Non-Crystalline Materials," (P. H. Gaskell, Ed.), Taylor & Francis, New York (1977).
3. T. Mori, S. Onari, and T. Arai, *Jpn. J. Appl. Phys.* **19**(6), 1027 (1980).
4. A. L. Renninger and B. L. Averbach, *Phys. Rev. B* **8**(4), 1507 (1973).
5. A. J. Leadbetter and A. J. Apling, *J. Non-Cryst. Solids* **63,** 250 (1976).
6. J. Notholt and J. Liese, *Phys. Status Solidi A* **114,** 207 (1989).
7. J. C. Phillips, *J. Non-Cryst. Solids* **34,** 153 (1979).
8. J. C. Phillips, *J. Non-Cryst. Solids* **43,** 37 (1981).
9. S. R. Elliot and A. V. Kolobov, *Philos. Mag. B* **61**(5), 853 (1990).
10. C. Carcaly and D. Houphouet-Boigny, *J. Non-Cryst. Solids* **86,** 271 (1986).
11. B. K. Teo, "EXAFS: Basic Principles and Data Analysis, Inorganic Chemistry Concepts 9," Springer-Verlag, New York/Berlin (1986).
12. K. Sakai, T. Koide, and T. Matsumoto, *Acta Crystallogr., Sect. B: Struct. Crystallogr. Cryst. Chem.* **B34,** 3326 (1978).
13. A. C. Stergiou and P. J. Rentzeperis, *Z. Kristallogr.* **173,** 185 (1985).
14. R. W. G. Wyckoff, "Crystal Structures," Vol. 1, 2nd ed. Wiley, New York (1965).
15. M. P. Fontana, P. P. Lottici, C. Razzatti, B. Bianchi, G. Antonioli, and U. Emiliani, *Solid State Commun.* **43**(7), 561 (1982).
16. C. Y. Yang, M. A. Paesler, and D. E. Sayers, *Phys. Rev. B* **39**(14), 10342 (1989).
17. P. Goldstein and A. Paton, *Acta Crystallogr., Sect. B: Struct. Crystallogr. Cryst. Chem.* **B30,** 915 (1974).
18. J. M. Lee, Ph.D. Dissertation, North Carolina State University at Raleigh, 1989 (unpublished).
19. M. Benfatto and C. R. Natoli, Unpublished versions of the CONTINUUM program for edge spectrum simulations.